Analyzing harmony and discord among optimal building controllers responding to energy, cost, and carbon reduction objectives

Lily X. Li[1,*], Gregory S. Pavlak[1,2]

The Pennsylvania State University, 104 Engineering Unit A, University Park, PA 16802, USA

Abstract

Optimization and control of building thermal energy storage holds great potential for unlocking demand-side flexibility, an asset that is being given much attention in current grid reforms responding to the climate crisis. As greater information regarding grid operations is becoming available, grid-interactive building controls inherently have become a multi-objective problem. Typical multi-objective optimization frameworks often introduce greater complexity and computational burden and are less favorable for achieving widespread adoption. With the overall goal of easing deployment of advanced building controls and aiding the building-to-grid integration, this work aims to evaluate the trade offs and degrees of sub-optimality introduced by implementing single-objective controllers only. We formulate and apply a detailed single-objective, model predictive control (MPC) framework to individually optimize building thermal storage assets of two types of commercial buildings, informed by future grid scenarios, around energy, economic, environmental and peak demand objectives. For each day, we compare the building's performance in every category as if it had been controlled by four separate single-objective model predictive controllers. By comparing the individual controllers for each day, we reveal the level of harmony or discord that exists between these simple single-objective problems. In essence, we quantify the potential loss that would occur in three of the objectives if the optimal control problem were to optimally respond to only one of the grid signals. Results show that on most days, the carbon and energy controllers retained most of the savings in energy, cost, and carbon. Trade-offs were observed between the peak demand controller and the other objectives, and during extreme energy pricing events. These observations are further discussed in terms of their implications for the design of grid-interactive building incentive signals and utility tariffs.

Keywords: model predictive control, grid-interactive buildings, thermal energy storage, controller dynamics, future grid scenarios

1. Introduction

The climate crisis calls for unprecedented efforts in reducing carbon emissions from all aspects of society. Demand-side flexibility, achieved with a highly integrated level of communication and coordination between the power supply and demand side, has been identified by recent studies as one of the key factors in the pathway towards carbon neutrality [1, 2]. While optimally controlled building thermal energy storage (TES) has been utilized for decades in providing various benefits, including load shifting [3, 4], reducing energy cost [5, 6], balancing fluctuation [7, 8, 9], reducing the size of battery storage [10], managing price volatility and uncertainty [11], and even reducing fossil-fired generation [12], adapting the traditional TES controls into a grid-interactive building control framework creates new challenges.

*Corresponding author

Email addresses: xml5187@psu.edu (Lily X. Li), gxp93@psu.edu (Gregory S. Pavlak)

[1]Department of Architectural Engineering

[2]Penn State Institutes of Energy and the Environment. He is also with the Department of Architectural Engineering.

The first challenge is clarity. Grid-interactive building control is inherently a multi-objective problem that is concerned with the building's performance in energy, economic, environmental, and demand flexibility categories. High-resolution grid-incentive signals, often at hourly or sub-hourly timescales, are increasingly being used as incentive signals in these grid-interactive building control models. The temporal variation within and across these signals amplifies the numerous possibilities for control strategies and further complicates the tradeoff dynamic between different aspects of building performance [13]. To make an informed control decision that satisfies the inherent nature of multi-objectivity, the ideal building control model needs to understand such dynamics, which may exhibit elements of harmony and discord among the control objectives. Typical *a priori* multi-objective optimization formulations, where a "weighting factor" is assigned to each objective to join all objectives into one function, falls short in this requirement. While it can provide a final solution to the problem that considers preferences among the objectives, this approach does not reveal insight into behind-the-scenes dynamics between the objectives and largely relies on the tuning of the "weighting factors."

The second challenge is simplicity. Implementing an advanced control algorithm, such as model predictive control (MPC), still proves to be time-consuming and complex in reality. Blum et al. [14] found that implementing a single-objective MPC controller that minimizes building electric power consumption in a real office building for roughly a month required 239 person-days equivalent of effort, which, in part points to the need for simplicity in formulating and solving the complex building control problem. The *a posterior* approach, another typical method in multi-objective problems, produces a pareto front that outlines a portfolio of solutions along with their objective values. Although much more information is presented regarding the trade-offs among objectives, this also creates additional complexity as someone or something (i.e., a multi-criteria decision algorithm) needs to make the final decision on the strategy that should be implemented.

Given this context, what the grid-interactive building control problem needs is a simple problem formulation that also provides clear, intuitive and easy-to-interpret insights into the dynamics between these building control objectives. Taking a step back from the typical multi-objective framework, this study attempts to tackle both challenges by an alternative approach. We formulate and apply a detailed single-objective, model predictive control (MPC) framework to individually optimize building thermal storage assets of two types of commercial buildings around energy, economic, environmental and demand flexibility objectives. For each day, we compare the building's performance in every category as if it had been controlled by four separate single-objective model predictive controllers. By comparing the individual controllers for each day, we reveal the level of harmony or discord that exist between these simple single-objective problems. In essence, we quantify the potential loss that would occur in three of the objectives if the optimal control problem were to only respond to one of the grid signals.

To complete this work, we utilize a novel grid dataset that was simulated for various future grid scenarios to frame the investigation in a forward-looking context. Section 2 provides additional context and reviews literature relevant to this study. Section 3 describes the methodology, including the reduced order building model, the formulation of the control problem and target metrics, and incentive signal profiles used for the MPC case study. Case study results are presented in Section 4. Limitations, conclusions and future work are discussed in Section 5.

2. Related Work

2.1. Building MPC Objectives and Incentive Signals

Building MPC is a powerful building optimization framework that develops optimal control strategies for a defined time period, "the planning horizon," into the future. Compared to traditional control approaches, MPC has the advantage of being forward-looking, as it solves a receding horizon optimal control problem by considering building information and using the current state of the system as the initial state [15]. It has also been favored for its ability to incorporate predictions of future disturbances and uncertainties, such as occupancy schedules and weather conditions, to achieve an optimal control outcome as in [16], [17] and [18]. For these reasons, the MPC framework has been widely applied in building optimal control research.

While there are sufficient studies using the MPC control framework in achieving a variety of building control objectives, existing work that utilizes the control of building thermal energy storage, both in single-objective and multi-objective formulations, has largely been focusing on the energy, economic and thermal comfort categories. Studies that focus on reducing energy consumption initially considered thermal comfort as the main constraint, such as in [19] and [20]. Other studies formulate their objective function to consider both energy consumption and thermal comfort at the same time. These include studies like [21], [22], [23], [24] among many others, all of which either formulated a comfort penalty into the cost function or treated both objectives separately to form a pareto front via multi-objective optimization.

As building control problems evolve with the growing diversity in the grid, the economic performance of a building or a portfolio of buildings is not simply an interest for building occupants and operators, but also an opportunity for researchers to explore the role of buildings in an integrated or "grid-connected" context. There are numerous studies that develop optimal control of building systems to support demand flexibility or economic objectives in the forms of load shifting, peak shedding and real-time signal following. Often, the MPC controller follows some type of economic incentive, such as electricity prices or demand charges, to generate an optimal control strategy that minimizes these economic targets. A few studies used artificial signals generated with a mathematical formula [20], while others used historic pricing information obtained from real electricity markets. For example, [25, 26, 27, 28, 29, 30] all developed an economic MPC model that uses historic electricity pricing signals for their MPC controller (in some cases, among other types of controllers) to search for an optimal control strategy for the building HVAC system that reduces building operational cost or peak electric demand in a more realistic context. More recently, studies have begun to investigate building TES for providing grid stability in microgrids with distributed PV and battery storage [7, 8, 9, 31].

One of the main limitations with these economic-oriented MPC studies is the incentive signals being used. While historic averages provide comprehensive information on how the grid behaved in the past, the increasing penetration of renewable energy and the shifting of peak demands and load profiles from building electrification is rapidly transforming the grid. Therefore, to generate accurate and informative optimization strategies for our buildings, it is imperative that advanced building control frameworks such as MPC are studied in the context of forward-looking energy system scenarios.

2.2. Quantifying Environmental Impact in Building MPC

Few existing MPC studies explored the environmental aspect of building performance, which can be partially attributed to the challenge of accurately quantifying the emissions related to electricity generation, and the relatively new and developing nature of this area. Average emission factors (AEFs), which describes the quantity of carbon released from one unit of generating electricity, are obtained by averaging total carbon emission over total electricity produced for a region over a period of time. This remains the most commonly adopted indicator used in building MPC studies. For example, Zhao et al. [32] used a fixed average emission factor for each generation technology in solving a MPC-based optimal scheduling problem considering distributed PV and storage systems. Vogler-Finck et al. [33] used average emission factor as the environmental incentive signal in their single-objective MPC optimization of a low-inertia heating system in a single-family residential building. Knudsen and Petersen [34] also used average emissions factor as the environmental incentive signal in their building MPC framework that considered both real-time pricing signal and carbon intensity in a multi-objective optimization setting.

Defined as the incremental change in carbon emissions incurred by an incremental change in the total electricity generated (or demanded), marginal emission factors (MEFs) have been used more prominently over the past several years to analyze the environmental impacts of a wide variety of actions that would alter the consumption or supply patterns of electricity. While AEFs quantify the total carbon emitted from generating electricity, the MEFs, which focuses on the marginal generator or technology, directly considers the response of the power system to a change in power consumption or generation. Studies by Hawkes [35] and Siler-Evans et al. [36] have argued that due to the often higher intensity of carbon emission of the generators at the margin, MEF is often higher than AEF and more adequate in capturing the dynamic change of carbon emissions. Studies have begun to leverage the advantage of MEFs to investigate the environmental impact of a wide range of objectives and programs. Using a simple conceptual model of demand response MEF, McKenna and Darby [37] argue that demand response technology and smart appliances create large carbon saving potential, especially when coupled with long-term structural change. Smith and Hittinger [38] used marginal emission factors to improve estimates of environmental benefits from appliance efficiency upgrades. Amoroso et al. [39] utilized the marginal emission factors to examine different sizing options and operating patterns of central air conditioning (AC) systems. Marginal emission factors were also adopted to evaluate emission benefits of building design implementations, such as increased insulation for new homes [40], and the long-term environmental performance of buildings designed to high performance standards [41]. As MEF signals become available at a high spatial and temporal resolution, studies have noticed the potentially volatile nature of the profile and the implication on the environmental impact resulting from demand response technologies. MEFs were used to reveal the high spatial and temporal dependency of carbon emissions from the charging behavior of electric vehicles (EVs) [42] and the importance of location in evaluating the environmental impact of renewable energy technology and efficiency-induced demand reductions [43].

Unfortunately, there are limited studies in the building MPC field that utilize MEFs. Péan et al. [44][45] were among the very few that calculated marginal emission factors for their MPC study using a regression model of average marginal emission rate as a function of load and the proportion of renewable energy resources. Although the regression model offered improvements over average emission factors, it was still limited in its spatial applicability.

2.3. Trade-off Dynamics in Single-Objective Building Optimizations

As briefly mentioned in Section 2.1, multi-objective optimization, both *a priori* and *a posterior* approaches, remains a common practice for incorporating multiple control objectives in building control work. Yet this practice is not without limitations. The *a priori* approach [22, 23], where a "weighting factor" is assigned to each objective to join all objectives into one function, only generates one solution which lacks information about the real trade-off dynamic happening behind the scenes. The *a posterior* approach [21, 24, 46], while providing a pareto front that outlines a portfolio of solutions and their objective values, often distracts the users who are left to make the final decision by themselves with too much information.

On the other hand, understanding the correlation or trade-off dynamics that could exist between these control objectives in a single-objective optimization context has become a more pressing issue recently when studies began to favor high-resolution grid incentive signals in building optimal controls, where the controller generates an optimal control strategy based on the hourly dynamics of the incentive signal. In these contexts, the consequences of optimizing around a single signal largely depend on whether the incentive signal used is "in-sync" or "out-of-sync" with other types of incentive signals. This effect has been investigated in a previous study [13], which reveals that even within each pricing signal cluster, which contains days that have very similar pricing signals, the average emission factors and marginal emission factors can be dramatically different from the pricing signal, and from each other. This study confirms that optimizing around one single signal without the knowledge of others may result in potential trade-offs among desirable control objectives.

While few researchers investigated this trade-off effect outside of the multi-objective pareto front approach, a few studies stand out. A 2015 study by Kircher and Zhang [47] reveals a trade-off effect among three types of demand flexibility MPC objectives. Specifically, optimizing around dynamic energy prices in a Large Office Building leads to some loss of benefit that can be unlocked via a controller formulated with a multi-tiered demand charge or formulated with a demand response program call. Knudsen and Petersen [34], who developed a building MPC framework that considers both real-time pricing signal and carbon intensity (again, using AEF as the incentive signal), attempted to quantify the trade-off dynamics between the environmental and economic objective by altering the "added weight" coefficient for the two objectives. The authors alluded to the importance of correlation between the two incentive signals; when they observed a stronger trade-off between the two objectives, the incentive signals were less correlated.

Péan et al. [45] applied a single-objective, MPC framework to a reduced-order model of a residential building, considering energy, economic and carbon emissions as the control objectives. Notably, the hourly pricing signal and marginal emission factors, calculated from a regression-based approach, used by the controller are out-of-sync most of the time. The results of this study revealed that different MPC objectives have different degrees of effect on the building's performance in the energy, economic, environmental and flexibility categories. Specifically, optimizing around carbon creates a trade-off with a 5% increase in both the cost and energy category, and reduces the level of demand flexibility; while optimizing around cost saves carbon and provides additional flexibility benefits, but increases energy consumption by 13%. More recently, Wang et al. [48] developed a rule-based, carbon-responsive control framework for a residential community. They observed that by optimizing around carbon emission, the energy consumption increased by 0.9% to 6.7%, while the change in energy cost was between -2.9% to 3.4% . While the focus of the study was not on the trade-off dynamic between objectives, the authors nevertheless affirm our intuition that trade-offs between grid-interactive building control objectives exist, especially when using high-resolution grid incentive signals.

2.4. Contribution

Existing studies have demonstrated the benefits and potential of the building MPC framework in optimal controls regarding energy, comfort and economic objectives. But there are several limitations that this study aims to address. First, only few studies explored the environmental performance of buildings and the impact of building demand response in the MPC framework. Most studies that did use the marginal emissions factor, like [45], calculated the signal from a regression-based model, rather than a detailed grid dispatch model. Second, most studies only addressed the building MPC problem from a reflective ("historical") and generalized perspective, using historic market data or emission factors averaged over a large region or timescale. Finally, very few studies have provided a comprehensive yet intuitive outlook on both the individual performance of various control objectives, and their trade-off dynamics in a single-objective optimization context. Indeed, current approaches to the multi-objective, grid-interactive building control problem are either time-consuming, such as the *a posterior* multi-objective pareto front, or lack substantial information about the trade-off dynamic, such as the *a priori* formulation based on "weighting factors".

To address these issues, this paper pays special attention to the incentive signals, and focuses on the analysis of signal dynamics and objective trade-offs. This study designs and implements a MPC control framework that optimizes around energy, economic, environmental and grid-support objectives separately. A newly-published grid operation dataset, built and simulated at the hourly timescale around various future grid scenarios, is used as the real-time, dynamic grid incentive signals [49]. We analyze the performance of these control objectives in two types of commercial buildings, each featuring a detailed HVAC system. Each building is optimized around four individual control objectives under the MPC framework for one month. The results of this study reveal the potential harmony or discord among grid incentive signals, and quantify the potential impact of implementing controllers that may only respond to one objective. The analysis provides insights into the complex tradeoff dynamic that exists among control objectives and the implications for developing intelligent building controllers that can support the transitioning electric grid.

3. Methods

The single-objective MPC framework was applied to two different commercial buildings over a month of operating time. For each building, four rounds of optimization were independently carried out to obtain the optimal setpoint schedule that minimizes each of the four MPC control objectives independently. The following sections describe the building models and their HVAC systems (Section 3.1), the MPC framework (Section 3.2), the formulation of the four objective functions (Section 3.3), the Cambium grid dataset (Section 3.4) and the grid incentive signals used in this study (Section 3.5), both hourly total energy price and hourly long-term marginal emissions rate.

3.1. Building Model Description

Building HVAC models and thermal zones were developed for a stand-alone medium office with a packaged direct expansion (DX) variable air volume (VAV) cooling system, and a large office building with a chilled water VAV system in Chicago, Illinois. Building parameters for the models are summarized in Table 1. The packaged DX VAV system consists of a VAV air handling unit with DX cooling coil, hot water heating coil, and dedicated outdoor air system (DOAS). Whereas the chilled water (CHW) VAV system of the large office building including chillers, cooling towers, water pumps, outdoor air economizer, and electric baseboard heating/reheat. All HVAC component models were based on the quasi-steady state physical formulations used by the EnergyPlus Engineering Reference Manual [50] and the ASHRAE HVAC Toolkit 2 [51].

The Reduced Order Model (ROM) used for simulating the thermal zone was developed based on an inverse grey-box thermal resistance-capacitance (RC) network. The building parameters used for the ROMs were identified from detailed EnergyPlus models for the two building types. The building model calculates hourly zone air temperature and zone electricity and energy load given the weather conditions, building parameters and setpoint schedules. For this study, the buildings were only simulated for the space cooling scenario for July. Both models (medium office and large office) have been validated in [52, 53]. Zone sensible load, temperature, and HVAC electric consumption are in fairly good agreement for both scenarios tested on the grey-box models.

Table 1: Building parameters for stand-alone medium office, and large office building energy models.

Parameter	Medium office	Large office	Units
Vintage	2001	1980	year
Floors	6	32	#
Volume	59,028	256,808	m^3
Conditioned Floor Area	14,240	76,659	m^2
U-value (no film)	0.334	0.339	W/m^2K
Internal Thermal Cap.	3788	19,043	MJ/K
Internal Thermal Cap./Area	266.0	248.4	MJ/Km^{-2}
Infiltration	0.13	0.17	ACH
Glazing Fraction	40	53	%
Glazing U-Factor	3.104	3.24	W/m^2K
Glazing SHGC	0.306	0.498	fraction
Lighting Power Density	7.164	9.8	W/m^2
Equipment Power Density	4.5	4.63	W/m^2
Occupant Density	18.58	51.81	m^2/person
HVAC System	DX-VAV	CHW-VAV	-
Chiller Rated Power	-	1960	kW
Chiller COP	-	4.4	-
CHW Pump Power	-	150	kW
CW Pump Power	-	150	kW
Cooling Tower Power	-	180	kW
AHU Rated Fan Power	200	815	kW
DX Rated Power	430	-	kW
DX COP	3.0	-	-
DOAS Rated Fan Power	14.4	-	kW

3.2. MPC Optimization Environment

A single building MPC environment in MATLAB, originally developed by [54] and extended by [3] was used as the basis for the single-objective optimization work in this study. For a defined planning period, the MPC environment couples building energy simulation with the optimization algorithm to find optimal building operational strategies (hourly zone air setpoint schedules) that minimize the desired objective value (e.g., energy, cost, or carbon emissions), in the presence of future grid operations (described in Section 3.4). For the single-objective case study, a variant of the metaheuristic particle swarm (PSO) algorithm was used as the optimizer.

For this study, the MPC model first establishes a baseline by calculating the objective value under the default building setpoint control strategy and weather conditions. Grid incentive signals from the novel dataset and other utility information are also loaded and used for calculating the objective value of energy cost and carbon emissions. After establishing a baseline, MPC initializes a warm up sequence that establishes a thermal history of the target building that can be prescribed and propagated through optimization iterations. Then, PSO begins the optimization process and searches for alternative setpoint strategies within the preset zone temperature setpoint constraints that minimize the objective function.

The process ends when the MPC model identifies a local minimum. Finally, the MPC model concludes by calculating the difference of the objective value between the baseline and the optimal solution.

3.3. Objective Functions

Four control metrics that quantify the energy, economic, environmental and peak demand penalty aspects of a building are formulated in this section. For this optimization problem, due to the nature of the PSO optimizer, the only constraint is the range of the setpoint temperature, described by a lower and an upper bound, the optimizer is allowed to choose from. For each round of simulation, the objective is to minimize the value of one of the four metrics. Although the simulation lasts for all twenty weekdays in the month of July, 2050 (using the calendar of 2012, to be consistent with the assumptions of Cambium), the MPC restarts each day with a planning horizon of 24 hours and does not consider the thermal history of the building as a result of optimal control from previous days. This was a deliberate decision to allow a fair comparison of the trade-offs between different building performance aspects as a result of different control objectives, on a day-to-day basis. If the thermal history from previous days were included, the initial building thermal state at which the MPC begins a new day of planning will vary across simulations, thus compromising the ability to make fair comparisons across the controllers for each day. Due to this reason, it is also worth acknowledging that the cumulative savings for each objective in this study will slightly vary from the actual savings that would be obtained in reality, where a building is continuously being optimized by an MPC controller for a month and previous days' control strategies have an impact on the building's thermal state at the beginning of each new operating day.

The energy metric quantifies a building's total electric energy consumption during the planning horizon as such,

$$E_{total} = \sum_{t=1}^{T} E_{use}(t) \tag{1}$$

where $E_{use}(t)$ is the total site electricity demand by the building over time interval t, where $t = 1$ and $T = 24$ in this case and includes lighting, equipment, and HVAC consumption. For the medium office building, E_{total} includes the electricity consumed by the DX-VAV fan, coil and the DOAS fan; for the large office building, it includes electricity consumed by the chiller, chilled water pump, cooling tower, and the AHU fan.

The cost metric is defined as the total energy cost that customers pay. E_{cost}, defined in Equation (2), states that

$$E_{cost} = \sum_{t=1}^{T} r(t) \cdot E_{use}(t) \tag{2}$$

where E_{cost} is the cost for total facility electricity consumption over the planning horizon; $r(t)$ is the energy pricing signal over time interval t, $E_{use}(t)$ is the electricity demand over time interval t, where $t = 1$ and $T = 24$.

For this study, marginal emission factors generated from the Cambium dataset were used as utility data to quantify the amount of carbon emission avoided by reducing electricity demand at the hourly level. Equation (3) formulates the objective function, C_{margin}, as a summation of the hourly change of carbon emission (kg) from the baseline due to the optimal control strategy. In detail, it states that

$$C_{margin} = \sum_{t=1}^{T} m(t) \cdot [E_{use,opt}(t) - E_{use,base}(t)] \tag{3}$$

where C_{margin} is the total change in the carbon emission over the planning horizon; $m(t)$ is the marginal emission factor over time interval t, $E_{use,opt}(t)$ is the electricity demand from the optimal case over time interval t and $E_{use,base}(t)$ is the electricity demand from the base case over time interval t. To find the optimal control strategy, the MPC model searches for the solution that has the smallest value of C_{margin}. A negative C_{margin} indicates that total carbon emission from the optimal case is lower than that from the base case.

The peak demand metric is used as the building demand flexibility metric in this study, by assigning a target demand limit (TDL) over a pre-defined window of peak building operation, and penalizing highest hourly exceeded amount with a penalty rate P. Equation 4, which states,

$$E_{dp} = max[P(max(window \cdot E_{use}(t)) - TDL), 0] \tag{4}$$

where P is the penalty rate applied to the peak hourly demand, $window$ is a vector that indicates the period of operation by assigning 1 to each hour where demand penalty is applied and 0 where it is not, $E_{use,base}(t)$ is the electricity demand from the base case over time interval t, and TDL is the target demand limit for the entire planning horizon. In reality, TDL and the penalty rate both depend on the location and electric market and should be adjusted accordingly. For the purpose of this study, an energy penalty is applied to the peak demand metric function using a user-selected weighting factor. A peak demand target at approximately 20% reduction of the baseline total building electric demand on the highest day of the month is applied.

3.4. Cambium Data Set

The source of the grid incentive signal largely affects the applicability and the interpretation of the MPC results. Most studies utilized the historical pricing data from a local electricity market. While more data were available at an hourly level, these historic data lack information of the actual marginal technology and only describes the grid operating in a reality from the past. Studies using these types of signals then produce results that can only be interpreted within that specific condition of the grid. As the penetration of renewable energy technology into the generation mix continue to increase every year, the grid dispatch becomes more dynamic and is less predictable from historical operational data. Under this reality, MPC of buildings should also be studied using a forward-looking approach, by utilizing modeled data sets that provide an outlook of the grid in the future.

The data set used for this study is generated by a novel grid operation model, "Cambium", developed by the National Renewable Energy Laboratory (NREL). NREL typically publishes a series of Standard Scenarios each year that describe scenarios of the U.S. power sector and grid operation in the future [55]. These scenarios outline the many possible outcomes of a future grid generation technology mix, predicted and categorized based on factors that have an impact on the grid, such as fuel price, technology advancements and so on. These Scenarios form the foundation of "Cambium", which assembles structured data sets of simulated hourly cost and operational data for modeled futures of the U.S. electric sector, with metrics designed to be useful for long-term decision-making. Drawing outputs from the Regional Energy Deployment System (ReEDS) model [56], a least-cost framework that projects structural changes in the U.S. electric sector under the Standard Scenarios, and the PLEXOS model [57], a commercial production cost model capable of simulating hourly operation of the future electric systems projected by ReEDS, "Cambium" employs a set of metrics to transform these outputs into structured data sets that describe a wide variety of grid operations at both busbar and end-use level, including detailed generation and capacity, marginal technology, detailed marginal electricity prices, and average and marginal emission factors [49]. All data from "Cambium" are detailed to the hourly level for every balancing area in the United States, from 2020 to 2050 in two-year increments and across several Standard Scenarios, which are updated every year as well. For example, "Cambium" version 2021 added datasets calculated for two new Scenarios specifically focusing on decarbonization efforts. Simulated based on possible future grid scenarios, "Cambium" allows opportunities for flexible planning and design that is based on the plausible realizations of the future. Utility data can be used to inform decisions and plannings for built environment and allows researchers to develop control strategies that are forward-looking.

3.5. Selected Grid Incentive Signals

Both the pricing signal and the carbon signal are generated from the "Cambium" dataset (2020 release) for the balancing area (BA) of Chicago for the year of 2050, under the Mid Case Scenario. This scenario serves as a baseline among the Standard Scenarios, where the total generation grows steadily over time and is provided primarily by a mix of new natural gas combined cycle (NGCC), PV, and wind generation.

There are a variety of marginal cost signals available from "Cambium", which are all estimates of the marginal costs induced by an increase in demand (or avoided costs from a decrease in demand). Conceptually, the marginal cost signal is similar to a day-ahead locational marginal price, and accounts for the cost of the effects of the generator short-run marginal costs, inter-BA transmission losses, the inter-BA transmission congestion and the distribution loss [49]. For this study, the marginal end-use energy cost, which describes the short-run cost for providing energy for a marginal increase in the end-use load, was selected as the pricing information for the MPC controller. Figure 1 shows the detailed hourly dynamics of the pricing signal from all twenty weekdays in the selected test month. In the original data, there are extreme pricing spikes that exceed \$2/kWh, which are likely due to the nature of modeled data. To create a more realistic context, a maximum of \$0.5/kWh was applied to these pricing signals, as shown in Figure 1. Other than a few days with these extreme spikes, the rest of the days in this simulation have relatively stable electricity prices, ranging from \$0.02 to \$0.07 per kWh.

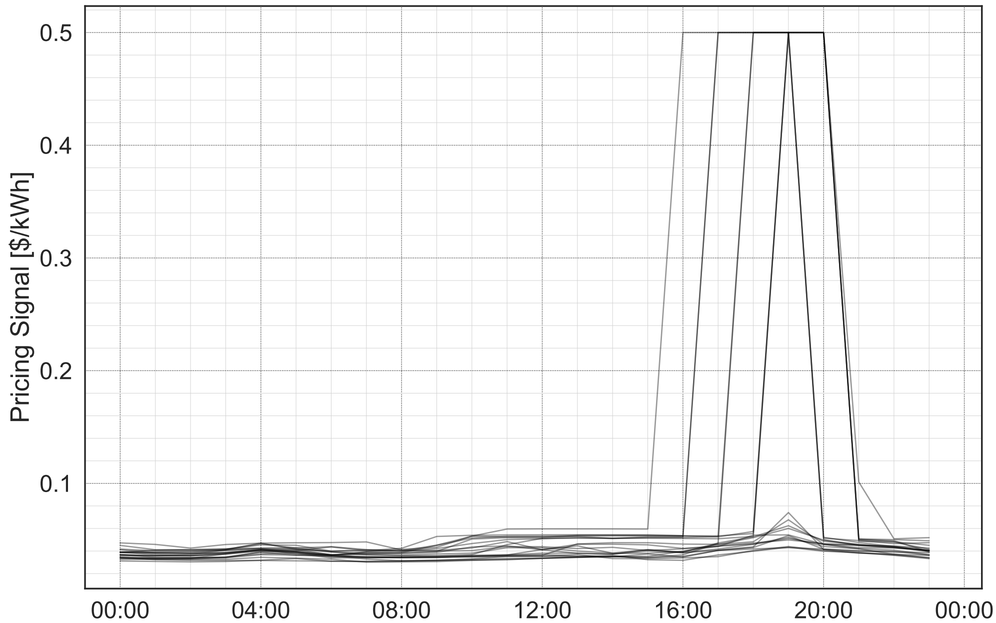

Figure 1: Selected pricing signals for the simulation month.

Similarly, the long-run marginal emission rate (LRMER) was selected as the carbon information provided to the MPC controller (i.e., m in Eq. (3)). LRMER is the marginal emission rate of the mixture of generation that would be either induced or avoided by a long-term change in end-use demand. While "long-run" does not refer to a specific number of years, LRMER treats the grid as ever-evolving by accounting for operational and structural changes that persist for years and is more preferable in quantifying long-term affect in emissions from persistent change in load [49]. More specifically, the LRMER is also levelized using methods from [58], which involves geographic aggregation across a few balancing areas and temporal levelization across a range of years while placing a greater weight on near-term years than years further out by applying time-value-of-money. This is recommended for works that specifically examine effects of measures and interventions planned for the future that will likely induce structural changes on the grid. Doing so will also allow the data to provide a good balance of capturing relevant regional effects while mitigating some of the issues that arise with attributing emissions to small geographic areas. Figure 2 outlines the hourly marginal emission factors for the simulation month. In general, the signal seems to favor the business-as-usual operation from commercial buildings, such that the lowest MEFs happen in the same time of the day with the highest electricity consumption.

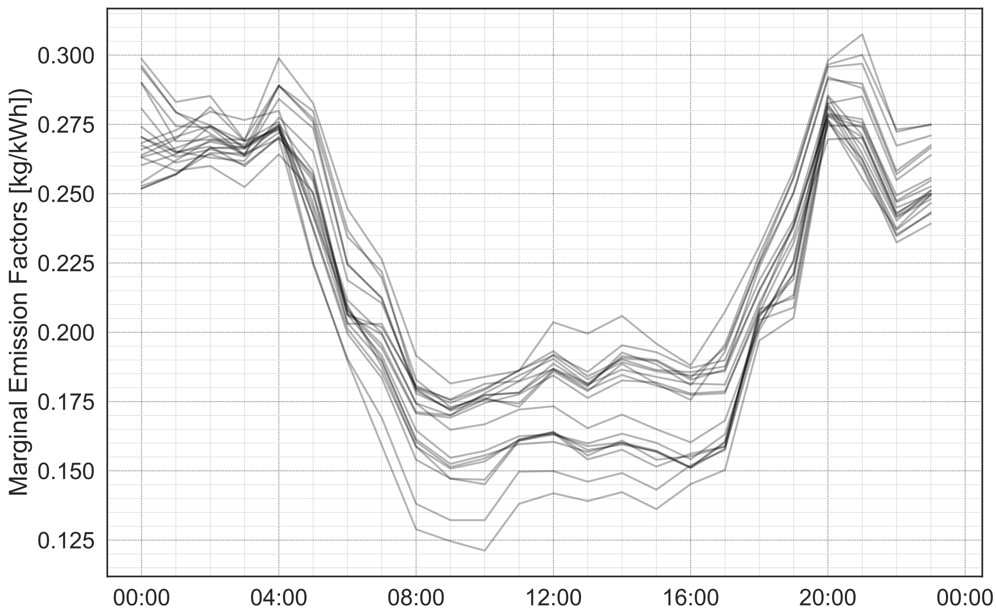

Figure 2: Selected carbon MEF signals for the simulation month.

4. Results and Discussion

The following sections summarize and highlight findings from the case study, in which the MPC framework was applied to optimize a medium office and a large office building. For each building, the MPC controller was given twenty days (all weekdays) to perform the optimization over four building control objectives. Section 4.1 outlines the day-to-day savings over the entire simulation period, and introduces the main graphs used to break down the individual and collective performance of each controller. Section 4.2 explores key factors that contribute to high savings from each control category. Sections 4.3, 4.4, 4.5 and 4.6 then explore key factors that contribute to the tradeoff and harmony between controllers by comparing days with the least and the most pronounced trade-off dynamics between control objectives.

4.1. Interpreting the Results Tables and the Loss Metric

Two figures will be referenced throughout the analysis to highlight day-by-day savings for all four controllers, in Table 2 for the Medium Office and Table 3 for the Large Office building. The Large Office building controller trade-offs and harmony are also highlighted by the loss metric in Figure 3. Both Figure 3 and Table 3 contain the same information for the Large Office building, but present different aspects of controller performance.

The result tables are primarily organized by the objective, also referred to as the controller, which is the target that the MPC controller was tasked with minimizing. Results under each objective are then categorized by four building performance metrics and the simulation date. In this way, information on both the savings of an objective as well as the subsequent effect of implementing that optimal strategy on other building performance metrics compared to the business-as-usual baseline performance are all included. The maximum saving for a particular objective, can be found under the objective section and then under the same metric name for a specific day; while the subsequent effect on the rest of the building performance metrics are found under different metric names. For example, according to Table 3, the maximum carbon savings via MPC on July 3rd for the Large Office building is 65.1 kg, and can be found under the objective section "carbon", and then at the intersection of the "carbon" sub-column and the date of interest. Further, on that same day, optimizing around carbon saved 2.4% of energy cost and 2.9% of total electric energy. The result tables are also color-coded given the magnitude of the value in each cell compared to the entire range of savings achieved from all four optimizations. All carbon savings are compared within their own range (for example, from 0 to 16.2 kg for the Medium Office and from 0 to 227 kg for the Large Office), while percent savings for the other three metrics were considered together. A color scale can be found at the bottom of Table 2 and Table 3 that explains this scaling method. Blue indicates a positive saving, while red indicates the metric is higher than that in the baseline (i.e. zero) "business-as-usual" operation. By comparing the shade of the colors, one can distinguish the magnitude of the benefits or trade-off effect from optimizing around a certain objective. For example, it is clear that optimizing around peak demand charges can cause significant increase in carbon emissions from the baseline, as demonstrated by the dark red shade of the "carbon" column under the "obj = peak demand" column on almost all of the days.

A loss metric is used to visualize the impact of a controller on other control metrics compared to the maximum available savings, obtained by optimizing around that control objective, also referred to as running that controller. Figure 3 presents the visualization of the loss metric for all four controllers in the Large Office building. Every row indicates the savings of one control metric, where each bar indicates the maximum savings obtained by that controller per day. The arrows indicate the reduction in that metric when another controller was used. For example, it can be read from the first row that on July 13, while the maximum carbon savings obtained by running the carbon controller is close to 160 kg, running the cost controller or the energy controller will lose some carbon savings, but still maintain a positive carbon emission reduction. On the other hand, running the peak demand controller will not only lose the entire carbon savings, but also increase carbon emission by more than 80 kg compared to the business-as-usual baseline operation. Thus, the loss metric highlights a controller's trade-offs with other controllers in the context of maximum available savings, whereas the result matrices highlights the trade-off dynamic with regards to the business-as-usual operation.

Table 2: Controller dynamic matrix for Medium Office Building

Controller	Carbon				Cost				Energy				Peak Demand			
Metric	Carbon [kg]	Cost [%]	Energy [%]	PD [%]	Carbon [kg]	Cost [%]	Energy [%]	PD [%]	Carbon [kg]	Cost [%]	Energy [%]	PD [%]	Carbon [kg]	Cost [%]	Energy [%]	PD [%]
7/3	7.1	1.5	1.6	0.4	7.1	1.5	1.6	0.4	7.1	1.5	1.6	0.5	-82	-3.2	-5.5	10.2
7/5	0	0	0	0	-7	0.1	0.1	0.6	-7	0.1	0.1	0.6	-74.8	-5	-6.3	10.5
7/6	0	0	0	0	-39.9	0.6	-3.9	-19.8	-7.9	0.2	0	0.6	-87.9	-0.2	-6.7	10
7/7	0	0	0	0	-76.3	3.8	-7.7	-25	0	0	0	0	-101	1.7	-7.6	11.9
7/10	3.4	0.9	1	0.4	3.4	0.9	1	0.4	3.4	0.9	1	0.4	3.4	0.9	1	0.4
7/17	16.2	1	1.6	0.6	15.5	1	1.6	1	16.2	1	1.6	0.6	-86.2	-3.3	-6.5	10.6
7/18	0	0	0	0	-82.3	0.9	-5.7	-16.8	-5.2	0.4	0.3	0.5	-101	0.2	-6.4	10.1
7/19	0	0	0	0	-8.6	0.2	0.1	0.6	-8.6	0.2	0.1	0.6	-77.2	-3.1	-5.8	10.7
7/20	0	0	0	0	0	0	0	0	0	0	0	0	-35.2	-4	-3.8	2.3
7/24	14.1	1	1.4	0.5	14.1	1	1.4	0.5	14.1	1	1.4	0.5	-106	-3.3	-6.7	13.7
7/26	0	0	0	0	0	0	0	0	0	0	0	0	-62.9	-2.9	-5.6	10.2
7/31	0	0	0	0	-3.4	0.1	0.2	0.5	-3.4	0.1	0.2	0.5	-16.2	-0.5	-1.1	2.4

carbon [kg]	:	-106	-26.5	0	4	16.2
cost/energy/PD [%]	:	-7.7	-2	0	3.4	13.7

4.2. Beginning Observations

This section provides an overview of the case study, highlights the different strategies used by the controllers and dives into selected days featuring some of the highest savings over the entire simulation period.

In general, comparing Table 2 and Table 3 reveals that the overall savings magnitude and potential, as demonstrated by the saving percentage and number of days with savings, are much higher for a Large Office building, compared to the Medium Office building. While the MPC only found four days with carbon savings and approximately half of the total simulation days with other savings in the Medium Office, the MPC found savings in all objectives on almost all of the simulation days for the Large Office. For simplicity, days that have zero savings in all four controllers have been removed from the Medium Office result matrix.

Table 3: Controller dynamic matrix for Large Office Building

Controller	Carbon				Cost				Energy				Peak Demand			
Metric	Carbon [kg]	Cost [%]	Energy [%]	PD [%]	Carbon [kg]	Cost [%]	Energy [%]	PD [%]	Carbon [kg]	Cost [%]	Energy [%]	PD [%]	Carbon [kg]	Cost [%]	Energy [%]	PD [%]
7/3	65.1	2.4	2.9	0	-138	2.6	2.7	0.8	-90.4	2.5	3.2	0.2	-1833	-6.7	-9.7	19.9
7/5	87.2	2.5	2.8	1.7	87.2	2.5	2.8	1.7	87.2	2.5	2.8	0.2	-1833	-10.6	-13.2	18.9
7/6	58.4	1.2	2.3	2	-313.7	3.3	-0.1	6.2	58.4	1.2	2.3	0.2	-1263	0.8	-9	18.5
7/7	138.2	1.5	3.3	5.5	-843.4	6.8	-5.7	-30	138.2	1.5	3.3	0.6	-2176	2.7	-15.2	21.2
7/10	1.4	0.2	0	2.9	-17.2	0.7	1.2	4.1	-128.2	0.6	1.3	0.5	-2084	-15.6	-14.1	20.3
7/11	0	0	0	0	-12.3	0.3	0.9	0.8	-12.3	0.3	0.9	0.1	-352.6	-3.4	-2	8.1
7/12	0	0	0	0	-75.3	0.4	0.2	5.5	-70.5	0.4	0.3	0.4	-372.4	-2.3	-2.4	8.8
7/13	154.5	2.1	2.5	-1	130.7	2.6	2.3	5.1	88.2	2.4	2.6	0.2	-84.3	0	-0.4	6.9
7/14	0	0	0	0	-58.5	0.5	0.5	5	-58.2	0.4	0.5	0.8	-58.2	0.4	0.5	8
7/17	141.3	2	2.7	1.8	1	2.7	3.2	3.4	80.8	2.4	3.3	0.3	-2135	-7.7	-14.7	21.5
7/18	227	3.1	3.9	0.6	-149	4.5	2	12.8	175.4	2.7	4.3	0.5	-1510	0.6	-11.2	20.1
7/19	155.7	1.9	3.4	0.6	155.7	1.9	3.4	0.6	155.7	1.9	3.4	0.1	-2139	-7.9	-15.9	18.7
7/20	78.4	2	2.6	0.2	78.4	2	2.6	0.2	78.4	2	2.6	0	-285.6	-2.6	-2.2	12.6
7/21	0	0	0	0	0	0	0	0	0	0	0	0	-33.7	-0.6	-0.6	1.3
7/24	66.1	1.7	1.8	-0.4	-414.6	3.5	0.6	11.7	-14.7	2.3	2.1	0.1	-2139	-5.9	-15	20.4
7/25	184.6	3.4	3.9	1.4	184.6	3.4	3.9	1.4	184.6	3.4	3.9	0.1	-461	-2.2	-1.2	10.4
7/26	0	0	0	0	-60.1	0.6	0.7	4.3	-60.1	0.6	0.7	0.4	-1844	-8	-15.4	19.1
7/27	71.8	2.4	2.3	2	71.8	2.4	2.3	2	71.8	2.4	2.3	0.2	-188	-1.4	-0.9	8.9
7/28	128.4	1.8	1.9	0.8	128.4	1.8	1.9	0.8	128.4	1.8	1.9	0.1	27.3	0.9	1.6	5
7/31	0	0	0	0	-293.7	0.6	-0.4	8.5	-32.5	0.5	0.6	0.1	-1565	-5.1	-11.6	15.5

carbon [kg]	:	-2176	-544	0	57	227
cost/energy/PD [%]	:	-30	-7.5	0	5.4	21.5

Table 4: Highest single day saving for Medium and Large Office

Objective	Medium office	Large office
Carbon	16.2 kg	227 kg
Cost	3.8%	6.8%
Energy	1.6%	4.3%
Peak Penalty	13.8%	21.5%

The MPC controller was also able to find a higher percentage savings in the Large Office building, compared to the Medium Office building, indicated by Table 4, which summarizes the highest savings achieved on a single day for every objective and both buildings. This is not surprising, considering the difference in the HVAC equipment between the Medium and Large Office building. Compared to the packaged DX VAV system in the Medium Office, the outdoor air economizer in the Large Office building can provide additional pre-cooling that allows the entire system to run more efficiently. This point can be further implied by the contrast in energy savings between the two buildings, which indicates the possibility that the economizer provided further energy savings. The thermal mass of the Medium Office building is also much lower, having only six floors, compared to thirty-two floors in the Large Office building. Both factors have a large impact on the total amount of savings that can be unlocked via optimal control of the building's passive thermal storage. Due to these reasons, the remaining discussions will focus on unpacking the savings of the Large Office building.

Figure 4 compares the optimal strategies and other aspects of building performance from days with the highest individual savings (see Table 4 for the exact values), which are July 18th (highest carbon and energy savings), July 7th (highest cost savings) and July 17th (highest peak penalty savings). For each day, the graph compares the mean air temperature, HVAC electric energy demand, grid incentive signals (if applicable) as well as the outdoor air temperature that allows detailed scrutiny into possible factors that contribute to high savings in each control category. The baseline control strategy, a typical scheduled

Figure 3: Loss metric for carbon, cost, energy and peak demand controllers

nighttime setup (therefore denoted as "NSU"), serves as the reference with no optimal control.

Different degrees and timing of pre-cooling can be observed by comparing the indoor air temperature

Figure 4: Comparison of mean air temperature, HVAC electric energy, grid incentive signals and outdoor air temperature on the days with the highest individual savings, July 18th (highest carbon and energy savings), July 7th (highest cost savings) and July 17th (highest peak penalty savings).

and the HVAC electric demand as a result of the optimal strategy used by each controller. In all four cases, signal dynamics play a central role in determining the optimal strategy and the charging and discharging of the passive thermal storage via pre-cooling activities. The marginal emission factors of July 18th, as seen in blue in the third row of Figure 4, align very well with the NSU HVAC electric demand profile, which means that the baseline NSU schedule is close to a carbon emission minimal schedule by itself. This also means that the MEF signal aligns quite well with the energy minimal strategy as well. For both the carbon and energy controller, the pre-cooling is mild, and takes place later in the early morning period, around 4 or 5 A.M., allowing a moderate amount of efficient "charging" in the cool morning to help reduce the start-up surge and save energy during the remaining hours of the day. In the case of the carbon controller, the system delayed start-up by an hour compared to the energy controller to reduce the high emissions rate at 4 P.M. Therefore, because the carbon signal aligns favorably with the energy controller, we observe a synergy between the two throughout the simulation period, and in particular on July 18th, when minimizing carbon saved 4% of energy as well, which is very close to the maximum available energy savings on that day at 4.3%.

On the other hand, signal dynamics of the cost and the peak demand controller encouraged an early and more aggressive start, as early as 2 A.M. at almost double the power of the energy controller, in the case of peak demand. Noticeably, both controllers have a second round of charging: for the cost controller, this happened at 2 - 3 P.M., to avoid the pricing peak at 4 P.M.; for the peak demand controller, this happened at 10 - 11 A.M., to avoid the peak penalty window from noon to 4 P.M. In the next sections, we will dive into the specific trade-off and harmony caused by each controller, elaborate on the tensions between them and potential solutions to alleviate these tensions.

4.3. Carbon Controller

The carbon controller, featured on the left most columns in the result tables and as the purple arrow in the loss metric, obtains as high as 227 kg of carbon savings in the Large Office building over the simulation period. The first observation from Table 2 and Table 3 is that optimizing around carbon almost always resulted in positive savings in other metrics, with the exception of July 13 and July 24, when optimizing around carbon caused a 1% and 0.4% increase in the peak demand metric. In addition, on days with generally low savings from all three objectives, such as July 10th, 11th, 12th, 14th, 24th, 26th and 31st, optimizing around carbon also has the lowest negative impact on other metrics. Referring to the first section in Table 3, we can observe that none of the optimal strategies (some of them are simply the baseline strategy) on these days caused a negative impact with cost or energy. But the opposite is not true. The second and third sections in Table 3, which show the results for the Cost and Energy objectives, respectively, reveal that on these low savings days, both the cost and the energy controller have a much larger negative impact on carbon, causing as much as 400 kg of increase in carbon emission.

In general, the carbon controller is a good surrogate for energy savings for this building. Referring to the third row of Figure 3, we observe that during six days (July 5, 19, 20, 25, 27 and 28), optimizing around carbon also produced the maximum energy and cost savings as well. On seven other days (July 3, 6, 7, 13, 17, 18, 24), optimizing around carbon causes very small loss in energy savings compared to the maximum savings on those days. Similarly, the carbon controller is a fair surrogate for cost savings as well. In addition to the seven days where optimizing carbon leads to maximum energy and cost savings, there are five additional days (July 3, 10, 13, 17, 18, 24) where optimizing around carbon only causes a small loss in cost savings.

While the carbon controller retains a substantial portion of the maximum energy and cost savings for two-thirds of the simulation period, there are a few days where the carbon controller loses the majority of the available savings, such as July 6 and 7 for cost and July 10 for energy. It also tends to lose most of the available savings for peak demand, although rarely causing an increase in peak demand either.

4.4. Energy Controller

The energy controller, highlighted by the third section in Table 3 and as the blue arrow in Figure 3, obtained as much as 4.3% of energy reduction on a single day. As discussed in previous sections, the key to energy savings is efficient pre-cooling available from the cool temperature in the late early morning period. These pre-cooling activities tend to be mild, compared to those favored by the cost and peak demand controllers. In general, the energy controller is in harmony with the carbon and cost metric and is a good surrogate for both. Like the carbon controller, which is in-sync with the energy controller, the energy-minimal strategy almost always saves carbon and cost, with some exceptions. This is supported by the fact that on 20% of the simulation days in the Medium Office (July 3, 10, 17 and 24), and 30% of all simulation days in the Large Office (July 5, 19, 20, 25, 27 and 28) the strategy to minimize energy is also the strategy that minimizes carbon and cost. We selected two of these days, July 19th and July 25th, which also features two of the highest carbon and energy savings over the entire simulation period, and compared their optimal strategy in Figure 5. We observe that both strategies are extremely similar and the key factor in achieving a triple-optimal solution lies in the energy savings, which was achieved from a mild amount of efficient "charging" at 5 AM that lowers the total energy use throughout the day. Cost did not become a major factor because the high price hours came after the end of occupancy when the HVAC systems were shut down and not able to be controlled. Therefore, we conclude that when the pricing, MEF and energy controllers are in-sync, such as on days presented in Figure 5, an energy-minimal strategy will lead to harmony in all three metrics.

In addition, the energy controller secures slightly more cost savings than the carbon controller, as seen on July 3, 10, 13, 14, 17, 24 and 31. But overall, optimizing around energy and carbon resulted in similar amount of cost savings, especially on high cost savings days.

On the other hand, optimizing around energy on low energy and carbon savings days creates tension with the carbon controller, such as on July 3, 10, 11, 12, 14, 24, 26, 31. Although both controllers rely on mild pre-cooling activities, the MEF signals, which only start to decrease at 5 A.M., is more likely to penalize pre-cooling activities that starts earlier than 5 A.M., which are used more often on low energy savings days to achieve efficient charging. To relieve this tension, one possible solution is to implement a minimal threshold for savings, which only allows the controller to opt for the optimal strategy if the energy savings is higher than a certain threshold, 1%, for instance.

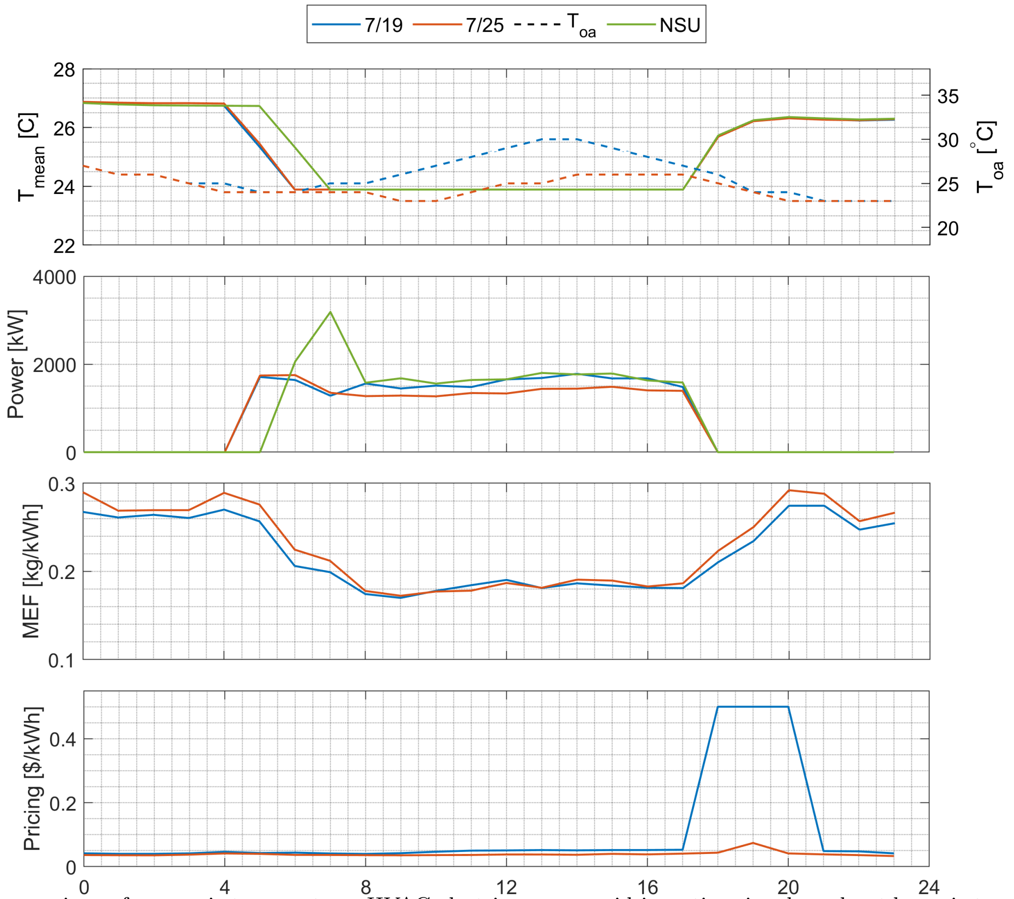

Figure 5: Comparison of mean air temperature, HVAC electric energy, grid incentive signals and outdoor air temperature on 7/19 and 7/25, the two days featuring an optimal solution that brings maximum savings in carbon, cost and energy categories.

4.5. Cost Controller

Observing the carbon column in the cost controller section in Table 3, we can easily see that optimizing around cost creates a negative impact on carbon more than half of the time. Comparing the cost savings on those days also reveals that such tension tends to take place on days with high cost savings, which are directly incentivized by the pricing spike in the late afternoon. Figure 6 highlights the details on two of such days, July 7th and July 24th, both featuring high cost and peak penalty savings, but a significant trade-off with carbon and energy. On the same day, the MPC controller makes very different decisions to save carbon and cost. Ultimately, this is largely determined by the dynamics between the MEF signal and the pricing signal. As discussed in the previous section, a pricing spike will strongly incentivize pre-cooling that is earlier (as early as 2 A.M.), in multiple waves (2 A.M., 5 A.M. and sometimes again around 1-3 P.M.), as well as in higher magnitude. This directly contrasts with the energy-conscious (a later start at 5 A.M.), moderate pre-cooling strategy that minimizes carbon emissions. These trends can be seen from the graph, which contrasts in the different starting time and peaks of use of the HVAC equipment. Given this, it is reasonable to conclude that in terms of the strategy adopted by the MPC controller, the signals are "in-sync" on days where the pricing spike occurs outside of occupancy/HVAC operation, and are "out-of-sync" when the pricing spike occurs during peak of afternoon HVAC operation. This almost entirely aligns with the trade-off dynamic observed in the results between the carbon and cost metric. Out of the eight days where the signals are "out-of-sync", six days (July 6th, 7th, 18th, 24th, 26th and 31st) feature the top worst trade-offs in carbon when MPC minimizes cost.

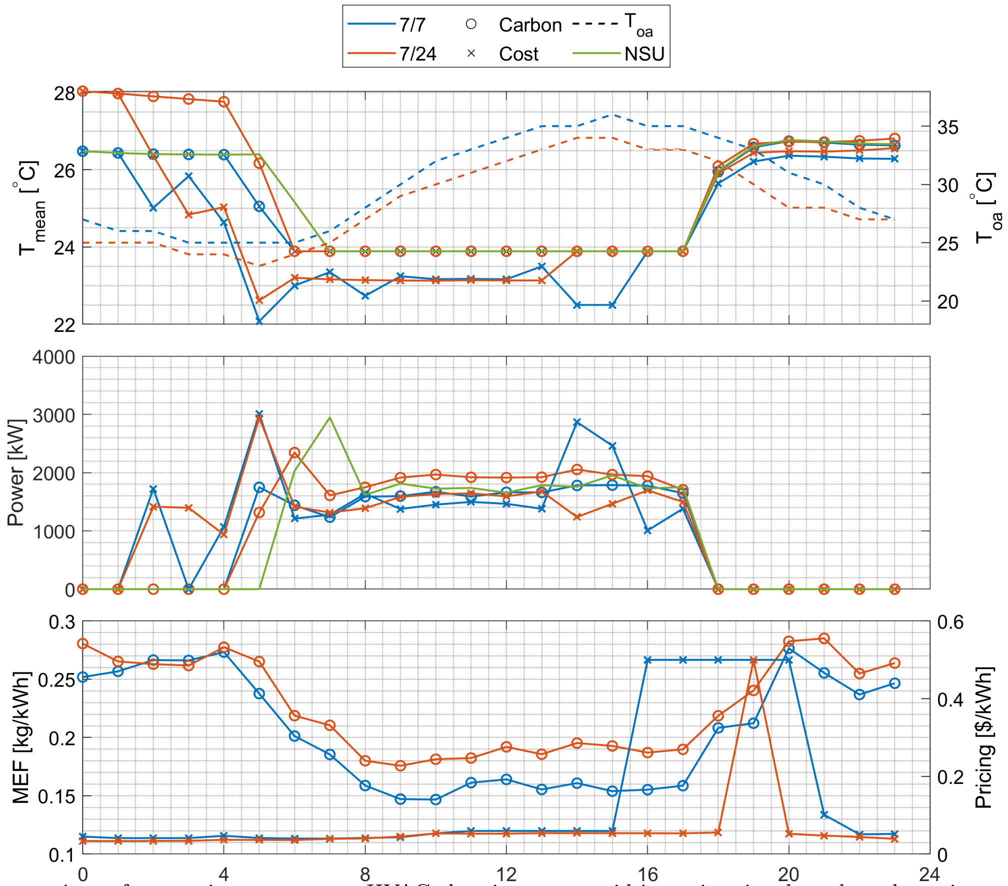

Figure 6: Comparison of mean air temperature, HVAC electric energy, grid incentive signals and outdoor air temperature on 7/7 and 7/24, the two days featuring the worst trade-off dynamic between the carbon and cost objective (optimal strategies for both objectives on both days featured on the graph)

The Cambium data set refers to these pricing spikes as a result of a lack of transmission capacity [49]. This could indicate that if these spikes were eliminated by separate measures, such as additional transmission and distribution capacity, the carbon and cost signals may be back in-sync again. In addition, the infrequent occurrences of these spikes may also suggest that the cost controller may only need to be used for these rare occasions, while the carbon or energy controller can be used for the majority of the building operation period.

4.6. Peak Demand Controller

The last observation is the interesting consequence of optimizing around peak demand penalty, which is often adopted by studies as a measure of demand-side flexibility. Based on the loss metric, even with an adjustable peak limit, which is set to approximately a 20% reduction in peak total building electric demand during the penalty window, and an adjustable energy penalty, the peak demand controller creates significant tension for carbon and energy savings, and only small harmony with cost on five days. The opposite is also true - while the carbon and energy controller rarely causes a negative impact on peak demand, both controllers nevertheless lose almost 100% of the available peak demand savings. The cost controller performs slightly better: when the prices drive the cost-optimal solution to pre-cool in a similar manner as the peak reduction case, we typically see half of the peak demand savings or more. The key of relieving this tension seems to be efficient charging. Currently, optimizing around peak demand rarely saves energy (only two days out of the entire simulation month), which as discussed in previous sections, is essential to achieving harmony among controllers. If the energy penalty is less severe, for this type of office building, the carbon penalty may reduce as well.

This result may indicate that the peak reductions should be limited to times that are necessary for managing grid reliability and future investment, rather than all the time, to relieve some of the tension with carbon or energy metric. It is also worth noting that under the current rate structure, which puts a heavy penalty on peak demand, even though reducing peak demand increases a building's total energy use, the total utility cost would likely still tend to go down because of the reduction in peak demand charges.

5. Conclusions

This research took a microscopic and forward-looking approach to model predictive control of building thermal mass energy storage systems. Innovative, high-resolution, future grid incentive signals were used by the model, which was applied to two types of commercial buildings for four independent control objectives over the course of one month. Analysis focused on the individual savings of each objective, as well as the harmony and discord among the objectives.

Grid-interactive building control is inherently a multi-objective problem. Results from this study reveal the different levels of benefit and potential pitfalls of optimizing around certain individual objectives. First and foremost, this study emphasizes the importance of using high resolution grid incentive signals, and the effect of signals being "in-sync" versus "out-of-sync" on the trade-off dynamic between different control objectives. For this particular study, both the carbon and the energy controller acted as a good surrogate for other metrics, frequently exhibiting the benefits of an energy minimization problem, although neither retained much of the available peak demand savings. The carbon controller also exerted minimal negative impact on other metrics while the energy controller retained slightly more of the maximum available savings of other controllers. A lower bound threshold might need to be implemented for the energy controller, to avoid a negative impact on carbon during low savings days.

Reducing peak demand can be important for reducing grid capacity and transmission/distribution investments. Reducing demand can also be important for avoiding system outages during extreme heat waves and/or cold snaps. Thus, there may be some need/benefit to having buildings reduce peak demand. Currently, if the buildings are incentivized to minimize their peak every month (e.g., as many current demand charges do), the operation may have negative consequences on carbon emissions and energy—unless sufficient efficiency gains can be realized during the load shifting process. If such efficiency gains cannot be realized, the peak reductions should perhaps be limited to times that are necessary for managing grid reliability and costly future investments, rather than all the time. A similar conclusion can be made for the cost controller. The tension between carbon and cost was mainly observed when the system was nearing generation capacity in the Cambium model, which produced large spikes in the marginal energy prices [49]. As building control decision-makers, we need to recognize the importance of having a cost-effective solution to address these pricing spikes while considering carbon emissions. Like the peak demand controller, if efficient charging cannot be realized, perhaps special attention should be paid to avoid exceeding grid capacity in the first place, among other measures to alleviate these pricing spikes. Fortunately, in the current Cambium mid-case model, the pricing spikes only occur on ten days in an entire year. If these pricing spikes cannot be addressed, decisions need to be made regarding whether to potentially sacrifice some carbon emissions for high cost savings on these small number of days. From an annual perspective, the potential increase in carbon emissions from responding to peak demand or high price events on a limited number of days should be greatly outweighted by the savings gained through minimizing energy use or carbon emissions on all other days.

Overall, if not all signals are available to buildings in the future, or if advanced control methods like MPC can only be applied to single-objective optimization problems due to the limit in time or computational resources, close attention should be given to the energy or carbon objective, both because of the dynamic and unpredictable nature of optimal solutions, but also its potential benefits to other building control objectives. For other objectives, such as cost or peak demand, perhaps it is not necessary to run the MPC on all days. In other words, developing controllers to optimize building operations primarily around energy or carbon, and then deviating only as needed to mitigate pricing spikes and grid constraints may be a reasonable strategy that keeps controller complexity low while enabling cost, carbon, and energy savings.

The concerted impact of signal dynamics, building type and environmental condition on the individual outcome of building MPC objectives and the collective harmony and discord between the control objectives are at the heart of the analysis. Future work that expands on the scope of this study should focus on these factors as well. For example, different conclusions may be drawn by implementing the same framework on residential buildings, which have somewhat of an opposite electric demand profile from a commercial building, or active thermal storage systems, which grants smaller buildings more storage autonomy. Results of this study also imply the potential of an electric market reform, which can drastically change the grid incentives available to building decision makers, and the structure under which building behavior is rewarded and penalized. As shown in this study, these changes may hold great potential in unlocking the full benefits of building demand-side flexibility via advanced controls.

Acknowledgements

Computations for this research were performed on the Pennsylvania State University's Institute for Computational and Data Sciences' Roar supercomputer. The authors would also like to thank Pieter Gagnon at The National Renewable Energy Laboratory (NREL) for an early access to the Cambium dataset, as well as his generous insights on the dataset.

References

[1] Larson E, Greig C, Jenkins J, Mayfield E, Pascale A, Zhang C, et al. Net-zero america: Potential pathways, infrastructure, and impacts, interim report. princeton university. 2020. URL: https://netzeroamerica.princeton.edu/the-report.

[2] Williams JH, Jones RA, Haley B, Kwok G, Hargreaves J, Farbes J, et al. Carbon-neutral pathways for the united states. AGU Advances 2021;2(1):e2020AV000284. URL: https://doi.org/10.1029/2020AV000284.

[3] Pavlak GS, Henze GP, Cushing VJ. Optimizing commercial building participation in energy and ancillary service markets. Energy and Buildings 2014;81:115–26. URL: https://doi.org/10.1016/j.enbuild.2014.05.048.

[4] Reynders G, Nuytten T, Saelens D. Potential of structural thermal mass for demand-side management in dwellings. Building and Environment 2013;64:187–99. URL: https://doi.org/10.1016/j.buildenv.2013.03.010.

[5] Henze GP, Felsmann C, Knabe G. Evaluation of optimal control for active and passive building thermal storage. International Journal of Thermal Sciences 2004;43(2):173–83. URL: https://doi.org/10.1016/j.ijthermalsci.2003.06.001.

[6] Greensfelder EM, Henze GP, Felsmann C. An investigation of optimal control of passive building thermal storage with real time pricing. Journal of Building Performance Simulation 2011;4(2):91–104. URL: https://doi.org/10.1080/19401493.2010.494735.

[7] Niu J, Tian Z, Lu Y, Zhao H. Flexible dispatch of a building energy system using building thermal storage and battery energy storage. Applied energy 2019;243:274–87. URL: https://doi.org/10.1016/j.apenergy.2019.03.187.

[8] Delgado MG, Ramos JS, Domínguez SÁ, Ríos JAT, Cabeza LF. Building thermal storage technology: Compensating renewable energy fluctuations. Journal of Energy Storage 2020;27:101147. URL: https://doi.org/10.1016/j.est.2019.101147.

[9] Miletić M, Schirrer A, Kozek M. Load management in smart grids with utilization of load-shifting potential in building climate control. In: 2015 International Symposium on Smart Electric Distribution Systems and Technologies (EDST). IEEE; 2015, p. 468–74. URL: http://10.1109/SEDST.2015.7315254.

[10] Swaminathan S, Pavlak GS, Freihaut J. Sizing and dispatch of an islanded microgrid with energy flexible buildings. Applied Energy 2020;276:115355. URL: http://www.sciencedirect.com/science/article/pii/S0306261920308679. doi:https://doi.org/10.1016/j.apenergy.2020.115355.

[11] Yu MG, Pavlak GS. Assessing the performance of uncertainty-aware transactive controls for building thermal energy storage systems. Applied Energy 2021;282:116103. URL: http://www.sciencedirect.com/science/article/pii/S0306261920315233. doi:https://doi.org/10.1016/j.apenergy.2020.116103.

[12] Langevin J, Harris CB, Satre-Meloy A, Chandra-Putra H, Speake A, Present E, et al. Us building energy efficiency and flexibility as an electric grid resource. Joule 2021;5(8):2102–28. URL: https://doi.org/10.1016/j.joule.2021.06.002.

[13] Li LX, Pavlak GS. Pattern analysis of dynamic grid incentives and the implications on optimal control of building thermal energy storage. In: International High Performance Buildings Conference. 2021, p. 1–10. URL: https://docs.lib.purdue.edu/ihpbc/391/.

[14] Blum D, Wang Z, Weyandt C, Kim D, Wetter M, Hong T, et al. Field demonstration and implementation analysis of model predictive control in an office hvac system. Applied Energy 2022;318:119104. URL: https://doi.org/10.1016/j.apenergy.2022.119104.

[15] Henze GP. Model predictive control for buildings: a quantum leap? 2013. URL: https://doi.org/10.1080/19401493.2013.778519.

[16] Oldewurtel F, Sturzenegger D, Morari M. Importance of occupancy information for building climate control. Applied energy 2013;101:521–32. URL: https://doi.org/10.1016/j.apenergy.2012.06.014.

[17] Killian M, Kozek M. Ten questions concerning model predictive control for energy efficient buildings. Building and Environment 2016;105:403–12. URL: https://doi.org/10.1016/j.buildenv.2016.05.034.

[18] Dong B, Li Z, Taha A, Gatsis N. Occupancy-based buildings-to-grid integration framework for smart and connected communities. Applied energy 2018;219:123–37. URL: https://doi.org/10.1016/j.apenergy.2018.03.007.

[19] Oldewurtel F, Parisio A, Jones CN, Morari M, Gyalistras D, Gwerder M, et al. Energy efficient building climate control using stochastic model predictive control and weather predictions. In: Proceedings of the 2010 American control conference. IEEE; 2010, p. 5100–5. URL: http://10.1109/ACC.2010.5530680.

[20] Zwickel P, Engelmann A, Gröll L, Hagenmeyer V, Sauer D, Faulwasser T. A comparison of economic mpc formulations for thermal building control. In: 2019 IEEE PES Innovative Smart Grid Technologies Europe (ISGT-Europe). IEEE; 2019, p. 1–5. URL: http://10.1109/ISGTEurope.2019.8905593.

[21] Li X, Malkawi A. Multi-objective optimization for thermal mass model predictive control in small and medium size commercial buildings under summer weather conditions. Energy 2016;112:1194–206. URL: https://doi.org/10.1016/j.energy.2016.07.021.

[22] Hazyuk I, Ghiaus C, Penhouet D. Optimal temperature control of intermittently heated buildings using model predictive control: Part i–building modeling. Building and Environment 2012;51:379–87. URL: https://doi.org/10.1016/j.buildenv.2011.11.009.

[23] Hazyuk I, Ghiaus C, Penhouet D. Optimal temperature control of intermittently heated buildings using model predictive control: Part ii–control algorithm. Building and Environment 2012;51:388–94. URL: https://doi.org/10.1016/j.buildenv.2011.11.008.

[24] Lauro F, Moretti F, Capozzoli A, Panzieri S. Model predictive control for building active demand response systems. Energy Procedia 2015;83:494–503. URL: https://doi.org/10.1016/j.egypro.2015.12.169.

[25] Oldewurtel F, Ulbig A, Parisio A, Andersson G, Morari M. Reducing peak electricity demand in building climate control using real-time pricing and model predictive control. In: 49th IEEE conference on decision and control (CDC). IEEE; 2010, p. 1927–32. URL: http://10.1109/CDC.2010.5717458.

[26] Hu M, Xiao F, Jørgensen JB, Li R. Price-responsive model predictive control of floor heating systems for demand response using building thermal mass. Applied Thermal Engineering 2019;153:316–29. URL: https://doi.org/10.1016/j.applthermaleng.2019.02.107.

[27] Ma J, Qin J, Salsbury T, Xu P. Demand reduction in building energy systems based on economic model predictive control. Chemical Engineering Science 2012;67(1):92–100. URL: https://doi.org/10.1016/j.ces.2011.07.052.

[28] Ma J, Qin SJ, Li B, Salsbury T. Economic model predictive control for building energy systems. IEEE; 2011. URL: http://10.1109/ISGT.2011.5759140.

[29] Bianchini G, Casini M, Vicino A, Zarrilli D. Demand-response in building heating systems: A model predictive control approach. Applied Energy 2016;168:159–70. URL: https://doi.org/10.1016/j.apenergy.2016.01.088.

[30] Aoki Y, Ito H, Ninagawa C, Morikawa J. Smart grid real-time pricing optimization control with simulated annealing algorithm for office building air-conditioning facilities. In: 2018 IEEE International Conference on Industrial Technology (ICIT). IEEE; 2018, p. 1308–13. URL: http://10.1109/ICIT.2018.8352367.

[31] Marušić D, Lešić V, Capuder T, Vasak M. Price-optimal energy flow control of a building microgrid connected to a smart grid. In: 2018 26th Mediterranean Conference on Control and Automation (MED). IEEE; 2018, p. 1–9. URL: http://10.1109/MED.2018.8443296.

[32] Zhao Y, Lu Y, Yan C, Wang S. Mpc-based optimal scheduling of grid-connected low energy buildings with thermal energy storages. Energy and Buildings 2015;86:415–26. URL: https://doi.org/10.1016/j.enbuild.2014.10.019.

[33] Vogler-Finck PJC, Wisniewski R, Popovski P. Reducing the carbon footprint of house heating through model predictive control–a simulation study in danish conditions. Sustainable Cities and Society 2018;42:558–73. URL: https://doi.org/10.1016/j.scs.2018.07.027.

[34] Knudsen MD, Petersen S. Demand response potential of model predictive control of space heating based on price and carbon dioxide intensity signals. Energy and Buildings 2016;125:196–204. URL: https://doi.org/10.1016/j.enbuild.2016.04.053.

[35] Hawkes AD. Estimating marginal CO_2 emissions rates for national electricity systems. Energy Policy 2010;38(10):5977–87. URL: https://doi.org/10.1016/j.enpol.2010.05.053.

[36] Siler-Evans K, Azevedo IL, Morgan MG. Marginal emissions factors for the us electricity system. Environmental science & technology 2012;46(9):4742–8. URL: http://dx.doi.org/10.1021/es300145v.

[37] McKenna E, Darby SJ. How much could domestic demand response technologies reduce CO_2 emissions? European Council for an Energy-Efficiency Economy 2017;URL: https://www.eceee.org/library/conference_proceedings/eceee_Summer_Studies/2017/2-policy-governance-design-implementation-and-evaluation-challenges/how-much-could-domestic-demand-response-technologies-reduce-co2-emissions/.

[38] Smith CN, Hittinger E. Using marginal emission factors to improve estimates of emission benefits from appliance efficiency upgrades. Energy Efficiency 2019;12(3):585–600. URL: http://10.1007/s12053-018-9654-4.

[39] Amoroso B, Hittinger E, McConky K. Keeping your cool–a multi-stakeholder look at ac sizing. Building and Environment

2018;131:306–29. URL: https://doi.org/10.1016/j.buildenv.2017.12.028.
[40] Levy JI, Woo MK, Tambouret Y. Energy savings and emissions reductions associated with increased insulation for new homes in the united states. Building and Environment 2016;96:72–9. URL: https://doi.org/10.1016/j.buildenv.2015.11.008.
[41] Collinge WO, Rickenbacker HJ, Landis AE, Thiel CL, Bilec MM. Dynamic life cycle assessments of a conventional green building and a net zero energy building: exploration of static, dynamic, attributional, and consequential electricity grid models. Environmental science & technology 2018;52(19):11429–38. URL: https://doi.org/10.1021/acs.est.7b06535.
[42] Zivin JSG, Kotchen MJ, Mansur ET. Spatial and temporal heterogeneity of marginal emissions: Implications for electric cars and other electricity-shifting policies. Journal of Economic Behavior & Organization 2014;107:248–68. URL: https://doi.org/10.1016/j.jebo.2014.03.010.
[43] Callaway DS, Fowlie M, McCormick G. Location, location, location: The variable value of renewable energy and demand-side efficiency resources. Journal of the Association of Environmental and Resource Economists 2018;5(1):39–75. URL: http://dx.doi.org/10.1086/694179.
[44] Péan T, Salom J, Ortiz J. Environmental and economic impact of demand response strategies for energy flexible buildings. In: 4th Building Simulation and Optimization Conference. Cambridge, UK; 2018, p. 277–83. URL: http://www.ibpsa.org/proceedings/BSO2018/3B-3.pdf.
[45] Péan T, Costa-Castelló R, Salom J. Price and carbon-based energy flexibility of residential heating and cooling loads using model predictive control. Sustainable Cities and Society 2019;50:101579. URL: https://doi.org/10.1016/j.scs.2019.101579.
[46] Yang R, Wang L. Multi-objective optimization for decision-making of energy and comfort management in building automation and control. Sustainable Cities and Society 2012;2(1):1–7. URL: https://doi.org/10.1016/j.scs.2011.09.001.
[47] Kircher KJ, Zhang KM. Model predictive control of thermal storage for demand response. In: 2015 American Control Conference (ACC). IEEE; 2015, p. 956–61. URL: http://10.1109/ACC.2015.7170857.
[48] Wang J, Munankarmi P, Maguire J, Shi C, Zuo W, Roberts D, et al. Carbon emission responsive building control: A case study with an all-electric residential community in a cold climate. Applied Energy 2022;314:118910. URL: https://doi.org/10.1016/j.apenergy.2022.118910.
[49] Gagnon P, Frazier W, Elaine H, Cole W. Cambium documentation: Version 2021. Tech. Rep.; National Renewable Energy Lab.(NREL), Golden, CO (United States); 2021. URL: https://www.nrel.gov/docs/fy22osti/81611.pdf.
[50] DOE . Energyplus engineering reference, the reference to energyplus calculations. 2013. URL: https://wem.lbl.gov/sites/all/files/engineeringreference.pdf.
[51] Brandemuehl M, Gabel S, Andresen I. Hvac 2 toolkit: Algorithms and subroutines for secondary hvac system energy calculations. atlanta: American society of heating, refrigerating and air-conditioning engineers. 1993.
[52] Henze GP, Pavlak GS, Florita AR, Dodier RH, Hirsch AI. An energy signal tool for decision support in building energy systems. Applied energy 2015;138:51–70. URL: https://doi.org/10.1016/j.apenergy.2014.10.029.
[53] Henze GP, Pavlak GS, Florita AR, Dodier RH, Hirsch AI. An energy signal tool for decision support in building energy systems. Tech. Rep.; National Renewable Energy Lab.(NREL), Golden, CO (United States); 2014. URL: https://www.nrel.gov/docs/fy15osti/63130.pdf.
[54] Corbin CD, Henze GP, May-Ostendorp P. A model predictive control optimization environment for real-time commercial building application. Journal of Building Performance Simulation 2013;6(3):159–74. URL: https://doi.org/10.1080/19401493.2011.648343.
[55] Cole WJ, Corcoran S, Gates N, Mai TT, Das P. 2020 Standard Scenarios Report: A U.S. Electric Sector Outlook. Tech. Rep.; National Renewable Energy Lab.(NREL), Golden, CO (United States); 2020. URL: https://www.nrel.gov/docs/fy21osti/77442.pdf.
[56] Brown M, Cole WJ, Eurek KP, Becker J, Bielen DA, Chernyakhovskiy I, et al. Regional energy deployment system (reeds) model documentation: version 2019. Tech. Rep.; National Renewable Energy Lab.(NREL), Golden, CO (United States); 2020. URL: https://doi.org/10.2172/1788425.
[57] Exemplar E. Plexos market simulation software. 2019. URL: https://energyexemplar.com/solutions/plexos/.
[58] Gagnon P, Frazier W, Elaine H, Cole W. Long-run marginal co2 emission rates workbooks for 2020 standard scenarios cambium data. Tech. Rep.; National Renewable Energy Lab.(NREL), Golden, CO (United States); 2021. URL: https://data.nrel.gov/submissions/170.